arXiv:cond-mat/9605188v2 31 May 1996

PERSISTENT CURRENTS IN INTERACTING ELECTRONIC SYSTEMS

Georges Bouzerar and Didier Poilblanc
Groupe de Physique Théorique, Laboratoire de Physique Quantique,
Université Paul Sabatier, 31062 Toulouse, France

Persistent currents in disordered mesoscopic rings threaded by a magnetic flux are calculated using exact diagonalization methods in the one-dimensional (1D) case and self-consistent Hartree-Fock treatments for two dimensional (2D) systems. For multichannel systems, a comparative study between models of spinless or spinfull (Hubbard) fermions has been done. First, it is shown that a purely one-dimensional model can not reproduce the correct order of magnitude of the observed currents. For 2D systems, going beyond first order pertubative calculations, we show that the second harmonic of the current is *strongly suppressed* in the case of spinless fermion models but *significantly enhanced* for the Hubbard model. This reduction (resp. increase) of the second harmonic is related to a strong increase (resp. reduction) of the spacial charge density fluctuations. Our work underlines the important role of the spin degrees of freedom in the persistent currents.

I. INTRODUCTION

The observations of mesoscopic currents in very pure metallic nano-structures was done in pioneering experiments [1–3]. In the first case, the experiment dealt with the average current of a system of 10^7 disconnected rings in the diffusive regime while, in the second, a single ring was used. Although the existence of such persistent currents in small metallic rings was predicted long ago [4,5], the magnitude of the observed currents is still a real challenge to theorists. Since studies neglecting electron-electron interaction do not reproduce the order of magnitude of the currents [6–9], there is a general belief that the interaction plays a crucial role in enhancing the current. It has been suggested that the currents could be enhanced to values close to the non disordered system case [10,11]. However, the exact role of the interaction in disordered systems is still unclear since treating interaction and disorder on equal footings is a difficult task.

II. 1D-SYSTEMS

Let us first consider the simplest case of pure 1D systems of spinless fermions. The hamiltonian of the model reads,

$$\mathcal{H} = -t/2 \sum_{<ij>} (exp(i2\pi\Phi/L) c^{\dagger}_{\mathbf{i}} c_{\mathbf{j}} + h.c.) + V \sum_{<ij>} n_{\mathbf{i}} n_{\mathbf{j}} + \sum_{i} w_{\mathbf{i}} n_{\mathbf{i}} \tag{1}$$

where L is the size of the system and $\Phi = \frac{\phi}{\phi_0}$, where ϕ is the flux through the ring and $\phi_0 = \frac{hc}{e}$. The third term describes the disorder, where $n_{\mathbf{i}} = c^{\dagger}_{\mathbf{i}} c_{\mathbf{i}}$ and $w_{\mathbf{i}}$ are on site potentiel chosen randomly in $[-W/2, W/2]$. The nearest neighbour interaction has an amplitude V.

If $E(\Phi)$ is the ground-state energy the persistent current is given by,

$$I = -\frac{1}{2\pi} \frac{\partial E}{\partial \Phi}. \tag{2}$$

An alternative to quantitatively estimate the persistent current is to calculate the Drude weight D,

$$D = \frac{L}{4\pi^2}[\frac{\partial^2 E}{\partial \Phi^2}]_{\Phi_m}. \tag{3}$$

Φ_m corresponds to the minimum of $E(\Phi)$. Using exact diagonalizations (ED) of small clusters by the Lanczos method [12], we have shown that, for strictly 1D systems [13] of spinless fermions, the effect of a *repulsive* interaction is to increase further the localization of the electrons and hence to decrease the value of the current. In fig.1 we have plotted the Drude weight as a function of the inverse system size for two different band-fillings. At half filling and for $W = 0$, the Mott transition can be easily seen from this picture. The transition from metallic to insulator occurs at $V_c = t$ (2t is the bandwidth). Away from half-filling and for $W = 0$, the system is always metallic and the Drude weight depends weakly on V. When disorder is switched on, for increasing repulsive interaction, we observe that D is reduced and, hence, the localization of the particles is increased. For $V > t$, the localization is both due to the Anderson localization and Umklapp processes generated by V. Note that, away from half-filling, we observe that the effect of V is very weak since Umklapp processes exist only in higher orders of the interaction. These results suggest that, for 1D systems of spinless fermions, the interaction do not counteract the effect of the disorder but, on the contrary, increases localization. Using a Hartree-Fock approach, Kato et al. [14] have obtained qualitatively good agreement with our ED results.

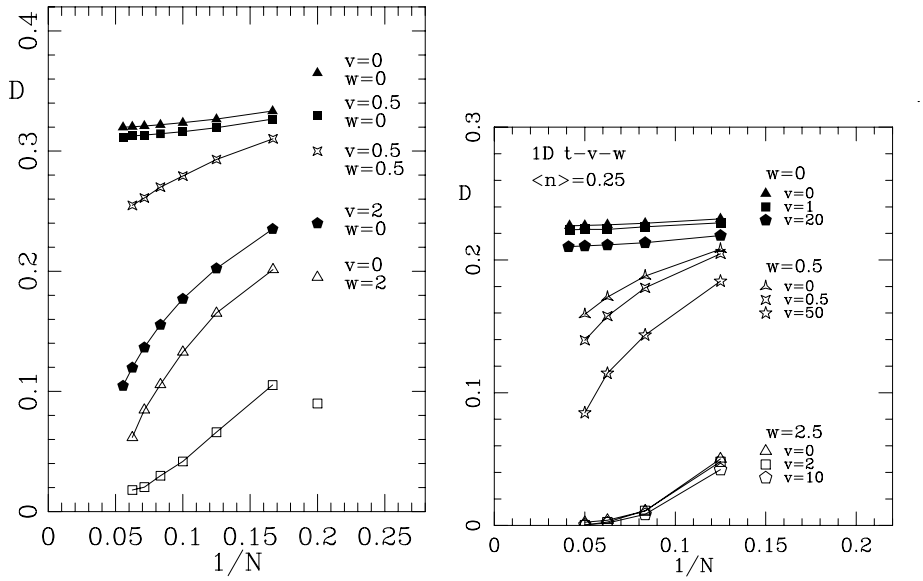

FIG. 1. Scaling of the Drude Weight at half-filling (right) and quarter-filling (left) vs inverse system size. The values of V and W (in units of t) are indicated on the picture. Each dot represents an average value over at least 300 configurations of the disorder.

The case of *attractive* interaction is generically very different. Indeed, for some values of the interaction parameters, the persistent currents can be increased, even in the presence of disorder. For the sake of simplicity, we shall concentrate here on the half-field case. At fixed V, the system exhibits a Kosterlitz-Thouless-like transition [15] at a critical value of the disorder parameter $W_c(V)$. In fig.2 we have plotted the phase diagram, calculated within a renormalization group (RG) approach, in agreement with ref. [16]. This picture suggests that for $-1 < \frac{V}{t} < -0.5$ the system is metallic for sufficiently weak disorder. Note that $W_c^{max} \simeq 2.3t$. For $\frac{V}{t} < -1$ and any filling, the system phase separates but this is of no interest for us in the present study.

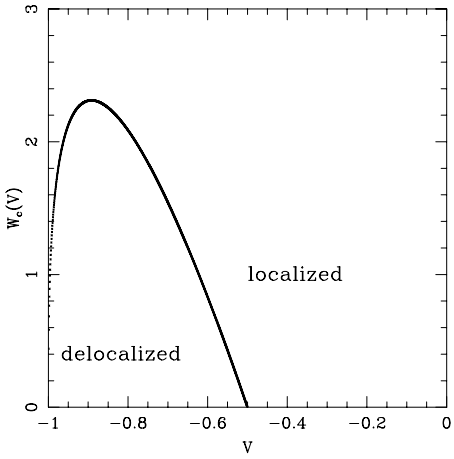

FIG. 2. Phase diagram $W_c(V)$ vs V obtained from an RG approach.

We have compared the ED and the RG results [17,18] and found a qualitatively good agreement. In fig.3 the Drude weight is plotted as a function of the inverse system size for various parameters V and W. For weak disorder $W < t$ the agreement is clear. However, our numerical data suggest that the delocalized region is restricted to a smaller part of the phase diagram. This minor discrepancy might be due to the fact that the RG approach neglects Umklapp processes and is perturbative in V.

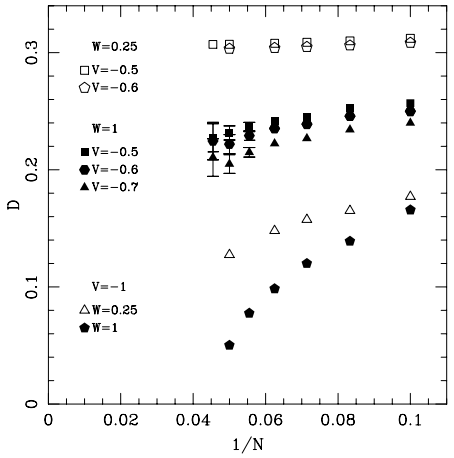

FIG. 3. ED results of the Drude weight vs 1/N for $V < 0$. Each dot represents an average value over at least 300 configurations of the disorder.

The difference between the repulsive and attractive cases can be understood in the following way: in the case of repulsive interaction the $2k_f$-fluctuations of the charge density are dominant. Therefore, the pinning by the impurity potential is strong and leads to a decrease of the localization length and, hence, to the reduction of the persistent currents. On the other hand, in the attractive case, the superconducting fluctuations are dominant.

For spinfull electrons (eg Hubbard model) Giamarchi et al. [19] have shown that the interaction, on the contrary, enhances the persistent current. In this case, the increase of the current is closely related to the *decrease* of the spacial charge fluctuations or, equivalently, to the smoothing out in space of the charge density. Indeed, for the repulsive Hubbard model, the spin density wave (SDW) fluctuations are dominant in the ground state (GS). On the other hand, for the attractive case, the spin fluctuations become gapped and thus pinning is favored. However, it should be noticed that, when $U \gg t$, the charge degrees of freedom can be mapped

onto a spinless fermion model with $k_f \to 2k_f$ [19] so that the $4k_f$ component of the disorder is expected to become important in this limit. At fixed W, we then expect a peak in the curve of D vs U. ED data on small Hubbard rings [20] have indeed shown such a behavior. More recently, RG calculations taking into account $4k_f$ scattering have also confirmed this assumption [21]. Second order perturbation calculations are also in good agreement with the ED results [22].

Even though repulsive Hubbard interactions increase the persistent currents, $4k_f$ scattering prevents the observation, in a strictly 1D system, of amplitudes of the order of the experimental data. It should also be stressed that models of spinless fermions in the continuum lead to opposite results [11]. Indeed, it has been argued that, in the case of 1D continuous models, a repulsive interaction can increase the persistent current up to values close to the 'clean' case. These results emphasize the important role of both the spin and the nature of the interaction on the lattice.

III. 2D-SYSTEMS

As stressed in the introduction, real experimental systems are 3D anisotropic materials. Moreover, a diffusive regime can only be realized in $d > 1$. A complete understanding of the persistent current phenomenon then requires the study of multi-channel systems. In section III, we shall present recent results concerning the effect of the electronic interaction for both spinless fermion and Hubbard multi-channel models [23,24]. Note that we shall focus only on the *second* harmonic I_{h2} of the current since (i) experimentally, in the multi-ring experiments, the current was found to be $\frac{1}{2}$ periodic and (ii) theoretically, it is well understood that the ensemble average (over filling or disorder) suppresses the first harmonic of the current [25,26,23].

Diagrammatic first order calculations (the spin is here irrelevant) have shown that the persistent currents are increased by the interactions [27]. More recently, Ramin et al. [28] have numerically shown by a Hartree-Fock (HF) approach, that the first order correction of the persistent current was in agreement with the analytical treatment [27]. In both spinless or spinfull models, the second harmonic is enhanced. However, a nearest neighbour interaction between spinless fermions tends to decrease the value of the *typical* current while a repulsive extended Hubbard interaction enhances it.

We have developped a self-consistent Hartree-Fock (SHF) method on finite lattices to treat the electron-electron interaction [23]. A systematic comparison with ED results on small lattices has revealed that this method was accurate even up to intermediate interaction strengths [23]. While, in the small coupling limit, the SHF method reduces to the HF method, at larger coupling it takes into account higher order powers of the interaction. Since the calculation is performed on (large) finite lattices quantum interferences due to the disorder potential are somehow treated exactly. It is important to note that this method is different from the usual perturbative scheme [27] where corrections to the current due to the electronic interaction are calculated perturbatively. Through the self-consistency relation, our procedure includes a resumation of higher order terms which becomes essential at moderate interaction strength. However, the direct relationship with a standard perturbative expansion remains unclear yet. Our study could be applied both to single or multi-ring experiments. ¿From a theoretical point of vue, the difference relies simply in the absence or presence of particle number fluctuations.

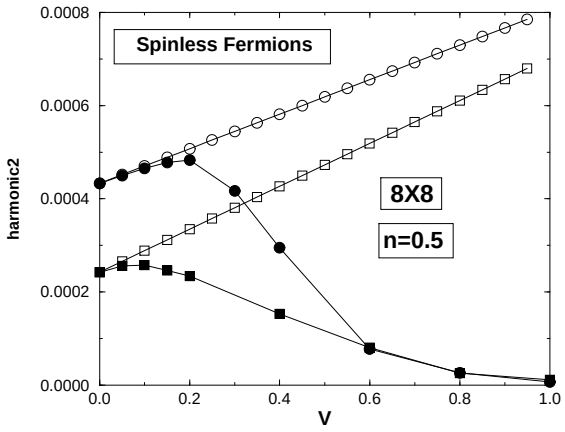

FIG. 4. $\langle I_{h2}\rangle_{dis}$ as a function of V calculated within the SHF method for spinless fermions on a 8×8 cylinder. An average over 1000 disorder configurations has been done. Comparison between first order HF (open symbols) and SHF results (full symbols) at half-filling. Circles correspond to $W = 3t$ and squares to $W = 4t$.

Section III is organized as follows: first, we compare, for both spinless and Hubbard models, the first order correction (in the interaction) and the SHF correction to the second harmonic of the persistent current. As expected, the two methods are in very good agreement in the small interaction limit. For larger interaction strengths, higher order corrections (taken care of in the SHF method) become important for the case of the spinless fermion model while they remain small in the Hubbard case. Secondly, we show that, as the interaction is switched on, the *decrease* (resp. *increase*) of the persistent current is always closely related to the *increase* (resp.*decrease*) of the charge density fluctuations. Lastly, a finite size analysis of the data of the second harmonic is performed.

The starting hamiltonian reads:

$$\mathcal{H} = \mathcal{H}_K + \mathcal{H}_{int} + \mathcal{H}_{des}. \tag{4}$$

$\mathcal{H}_K$ is the usual kinetic part containing the flux dependance, $\mathcal{H}_{des}$ is the term due to the disorder,

$$\mathcal{H}_{des} = \sum_{\mathbf{i}} w_{\mathbf{i}}\, n_{\mathbf{i}}. \tag{5}$$

The sites $\mathbf{i}$ are now chosen on a $L\times L$ lattice with periodic boundary conditions in one direction. The disorder parameter W is restricted to a finite interval for which the (non-interacting) system is as close as possible to a diffusive regime [29]. $\mathcal{H}_{int}$ is the interacting part, where, in the Hubbard case, $n_{\mathbf{i}} = n_{\mathbf{i}\uparrow} + n_{\mathbf{i}\downarrow}$. In the spinless fermion case,

$$\mathcal{H}^S_{int} = V \sum_{\mathbf{i},\mathbf{j}} n_{\mathbf{i}}\, n_{\mathbf{j}}, \tag{6}$$

where $\mathbf{i},\mathbf{j}$ stand for nearest neighbour sites and V is the strength of the screened interaction. In the Hubbard case, the interaction part is local in space,

$$\mathcal{H}^H_{int} = U \sum_{\mathbf{i}} n_{\mathbf{i}\uparrow}\, n_{\mathbf{i}\downarrow}. \tag{7}$$

In the SHF approximation, a mean-field type of decoupling is performed,

$$\mathcal{H}^S_{int} = -\sum_{\mathbf{i,j}} \delta t_{\mathbf{ij}}\, c^\dagger_{\mathbf{i}}\, c_{\mathbf{j}} + \sum_{\mathbf{i}} \delta w_{\mathbf{i}}\, n_{\mathbf{i}} - \frac{1}{2}\sum_{\mathbf{i,j}} V_{\mathbf{ij}}\,(\langle n_{\mathbf{i}}\rangle\langle n_{\mathbf{j}}\rangle - \left|\,\langle c^\dagger_{\mathbf{j}}\, c_{\mathbf{i}}\rangle\,\right|^2) \tag{8}$$

which renormalizes the on-site disorder term (Hartree term) $\delta w_{\mathbf{i}} = \sum_{\mathbf{j}\neq\mathbf{i}} V_{\mathbf{ij}}\langle n_{\mathbf{j}}\rangle$ and the hopping term (Fock term) $\delta t_{\mathbf{ij}} = V_{\mathbf{ij}}\langle c^\dagger_{\mathbf{j}}\, c_{\mathbf{i}}\rangle$. The quantities $\langle n_{\mathbf{j}}\rangle$ and $\langle c^\dagger_{\mathbf{j}}\, c_{\mathbf{i}}\rangle$ have to be determined self-consistently. Similarly, $\mathcal{H}^H_{int}$ becomes,

$$\mathcal{H}^H_{int} = U\sum_{\mathbf{i}}(\langle n_{\mathbf{i}\uparrow}\rangle\, n_{\mathbf{i}\downarrow} + \langle n_{\mathbf{i}\downarrow}\rangle\, n_{\mathbf{i}\uparrow} - \langle n_{\mathbf{i}\downarrow}\rangle\langle n_{\mathbf{i}\uparrow}\rangle). \tag{9}$$

For simplicity the calculations have been done in the paramagnetic sector (i.e. $\langle n_{\mathbf{i}\downarrow}\rangle = \langle n_{\mathbf{i}\uparrow}\rangle$). In this case the spin $\uparrow$ and $\downarrow$ are decoupled,

$$\mathcal{H}^H_{int} = \sum_{\sigma} \mathcal{H}^\sigma_{int} \tag{10}$$

where,

$$\mathcal{H}^\sigma_{int} = U\sum_{\mathbf{i}}(\langle n_{\mathbf{i}\sigma}\rangle n_{\mathbf{i}\sigma} - \frac{1}{2}\langle n_{\mathbf{i}\sigma}\rangle^2). \tag{11}$$

Note that, due to the disorder potential, the various mean-field quantities are space dependent so that a numerical investigation on a finite lattice is necessary. Similar equations also hold in the HF approximation but, in this case, the expectation values are simply taken in the non-interacting GS.

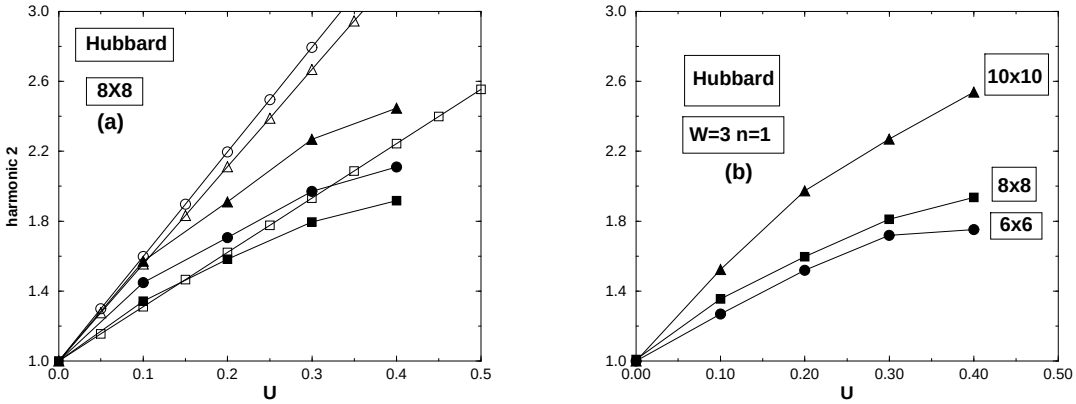

FIG. 5. (a) (a) Ratio $\langle I_{h2}\rangle_{dis}(U,W)/\langle I_{h2}\rangle_{dis}(0,W)$ as a function of U calculated in the Hubbard model within both HF (open symbols) and SHF (full symbols) methods on a 8×8 cylinder. Circles correspond to $W = 3t$ at quarter-filling, squares to $W = 3t$ at half-filling and triangles to $W = 4t$ at half-filling. (b) Same as (a) at fixed $W = 3t$ and at half-filling for several system sizes.

Since the current is periodic of period 1 (in units of Φ_0), it can be expanded as a Fourier series,

$$I(\Phi) = \sum_{\mathbf{n}} I_{hn}\, sin(2\pi\, n\Phi), \tag{12}$$

where I_{hn} are the harmonics of the current. In fig.4 we have plotted $\langle I_{h2}\rangle$ ($\langle\rangle$ means average over disorder) at half-filling, for a 8×8 system, as a function of V. $\langle I_{h2}\rangle$ is calculated by averaging

over at least 1000 configurations of the disorder. As expected, we observe for weak values of the interaction a perfect agreement between the SHF and the HF calculations. However, as we increase V, the SHF results show a strong reduction of the current while the HF results predict an increase. We also observe that the region of agreement between HF and SHF methods is reduced as the disorder increases. This means that, as the strength of the disorder increases, higher order corrections in the interaction become significant and, thus, a first order calculation is not sufficient. We will see later on that this reduction is related, as in the 1D case, to an increase of the charge density fluctuations. Using the SHF method, we have checked that this effect persists for larger system sizes and away from half-filling. In conclusion, the repulsive interaction are detrimental to the persistent currents in spinless fermion models with short range interactions. Note however that, in a different regime, for much *stronger* disorder, an enhancement of the persistent currents by the interactions has been found [30].

However, a different behavior is observed in the case of the Hubbard model as seen in fig.5, showing the relative effect of the interaction on the current, i.e. $\frac{\langle I_{h2}\rangle_{(U,W)}}{\langle I_{h2}\rangle_{(0,W)}}$. Fig.5(a) reveals that both SHF and HF calculations predict an increase of the current and that the first order calculation gives relatively good results. It is interesting to note that the first order calculations always give higher values of the currents. In Fig.5(b), we have plotted the same quantity, for a fixed density, but for different system sizes. It clearly indicates that, as the size of the system increases, the effect of U becomes stronger.

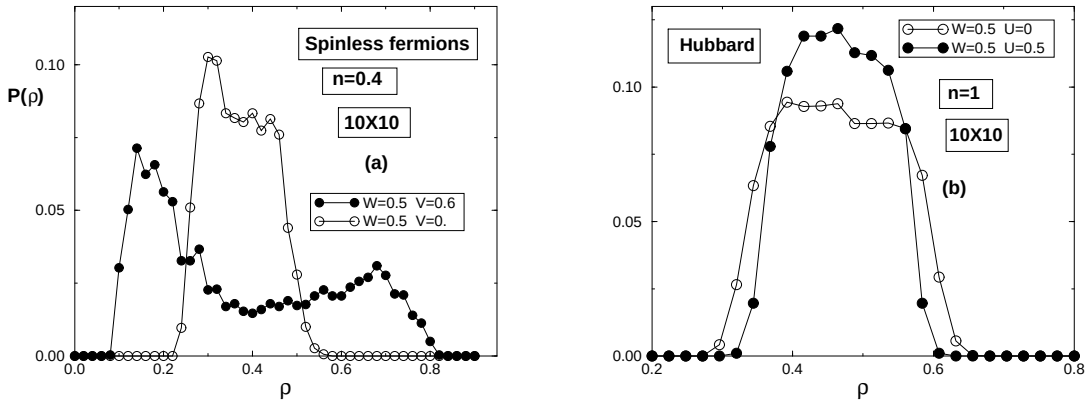

FIG. 6. Distribution $P(\rho)$ in both spinless fermion (a) and Hubbard (b) models, for a 10×10 cylinder, and different band fillings n. The values of V, W and U are indicated in the figures. An average over 30 configurations of the disorder has been performed.

At this point, these first results suggest the importance of the nature of the interaction. Indeed, in the spinless case, the currents are strongly reduced by the interaction while, on the contrary, the Hubbard repulsive interaction enhances the currents. In addition, it has been shown that in the spinless fermion case, higher order terms become rapidly dominant even for relatively modest values of the interaction strength so that a simple HF approach is not sufficient.

Let us now try to build up a physical picture of this phenomenon. The distribution of the local charge density $n_{\mathbf{i}}$ turns out to be directly connected to the localization. Considering many configurations of disorder (labeled by some integer k), we assume that the related local site densities $n_{\mathbf{i}}^k$ (where the subscript k stands for the disorder configuration) are independent realizations of a statistical variable ρ. In fig.6 we have plotted the distribution of the local density ρ for spinless fermion (a) and Hubbard (b) models. We clearly observe that the shape

of the distribution changes with the interaction. In the spinless fermion case, two peaks clearly appear. This suggests the existence of two categories of sites with rather large and small charge densities, respectively. On the contrary, in the Hubbard case (b), we observe that the interaction has now the opposite effect i.e. the distribution shrinks around the average value. In other words, the interaction tends to homogenize the charge density in space.

Let us now turn to more qualitative results. For this purpose, let us define,

$$\delta\rho_k = \sqrt{\frac{1}{L^2}\sum_{i=1}^{L^2}(\langle n_i^k\rangle - n)^2} \tag{13}$$

and,

$$\delta\rho = \frac{1}{N_{cdes}}\sum_{k=1}^{N_{cdes}}\delta\rho_k \tag{14}$$

where L is the length of the system, N_{cdes} is the number of disorder configurations, and $\langle n_i^k\rangle$ are calculated self-consistently. We expect, for big systems, $\delta\rho_k$ to become independent of the disorder configuration. Results for $\delta\rho$ vs U or V are plotted in fig.7 for various fillings. For spinless fermions, it appears that $\delta\rho$ increases with V at any fillings. For example, for $n = 0.4$, the width increases by almost a factor 4 at $\frac{V}{t} = 0.8$. However, in the Hubbard case, the effect of U is just the opposite e.g. the reduction of $\delta\rho(U, W)$ is larger than 25% at half filling. Note that, in general, the magnitude of the effect (relative increase or decrease with the interaction) increases with the density, as commensurability is approached.

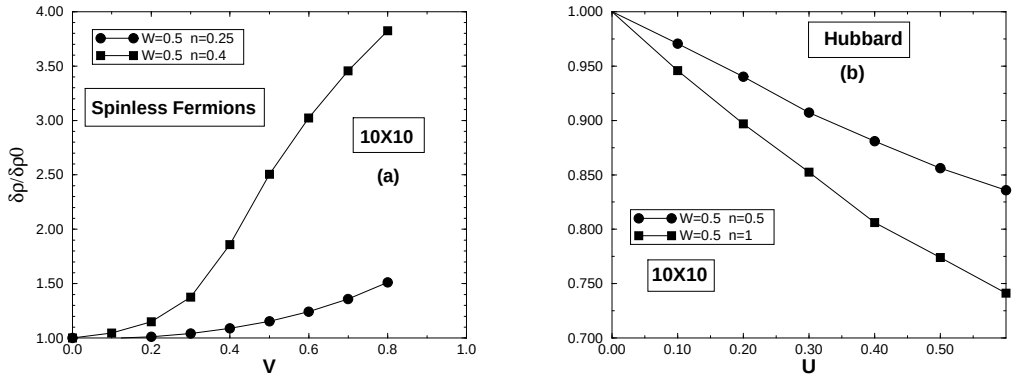

FIG. 7. Ratio $\delta\rho(VU, W)/\delta\rho(0, W)$, (VU is V or U) as a function of the interaction parameter (U or V) for different filling factors n. The calculations have been done on a 10×10 cylinder with 30 configurations of the disorder.

To finish, we now turn to dependence of the width of the distribution $\delta\rho$ on the disorder parameter W summarized in Fig.8. As expected, for vanishing interaction strength, the distribution of the local densities increases almost proportionnaly with W. For finite interaction, Fig.8 shows that the *sign* of the effect observed depends only on the nature of the interaction (U or V) and not on the disorder. The magnitude of the increase/decrease seems to depend roughly on the combination $\frac{V}{W}$ or $\frac{U}{W}$.

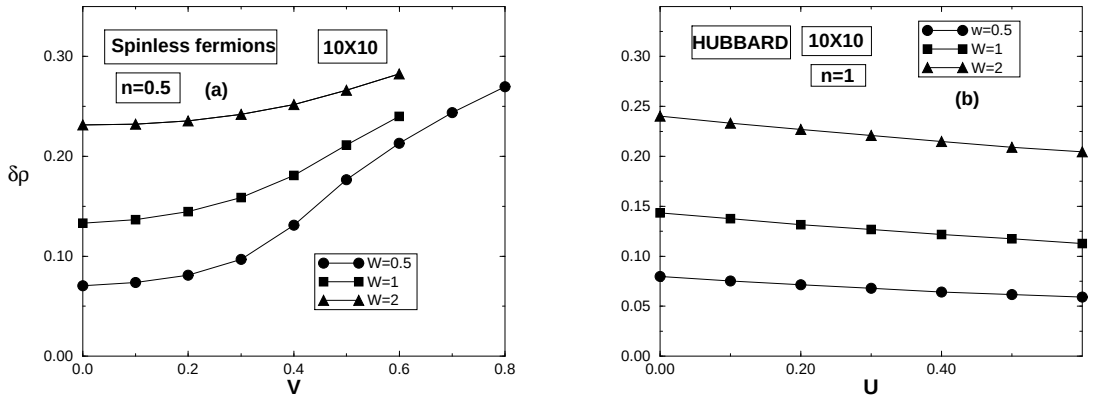

FIG. 8. $\delta\rho(V or U, W)$ as a function of the interaction parameter (V or U) for different disorder W/t. The calculations have been done on a 10×10 cylinder with 30 configurations of the disorder.

IV. CONCLUSION

In conclusion, we have presented data beyond first order perturbative calculations. In 1D, exact diagonalisation data clearly show that the electronic interaction enhances localization. In 2D, a self-consistent mean-field treatment of the interaction is used for the first time in the case of disordered fermions on a lattice. The SHF method has proven itself to be a good tool to study the effect of the interaction for $d > 1$. It provides strong evidences that spinless and spinfull fermions behave differently. The above SHF results show that the increase of the persistent current is strongly connected to the spin degrees of freedom. Although the calculations presented here concern 2D systems, we expect that, for bigger systems and higher connectivity, the pinning with the impurities becomes weaker. However, quantitative data are still missing for realistic mesoscopic sizes and more work is certainly needed to know whether such models can account for the correct magnitude of the experimentally observed current.

D.P. acknowledges support from the EEC Human Capital and Mobility Program under grant CHRX-CT93-0332. *Laboratoire de Physique Quantique (Toulouse)* is *Unité Mixte de Recherche No. UMR5626 du CNRS*. We thank IDRIS (Orsay, France) for generously providing CPU time on the C94 and C98 supercomputors.

---

[1] L.P. Levy, G. Dolan, J. Dunsmuir and H. Bouchiat, Phys. Rev. Lett. **64**, 2074 (1990).
[2] V. Chandrasekhar, R.A. Webb, M.J. Brady, M.B. Ketchen W.J. Galager, and A. Kleinsasser, Phys. Rev. Lett. **67**,3578 (1991).
[3] D. Mailly, C. Chapelier, and A. Benoit, Phys. Rev. Lett. **70**, 2020 (1993).
[4] N. Byers and C. N. Yang, Phys. Rev. Lett. **7**, 46 (1961); W.Kohn, Phys. Rev. **133**, A171 (1964).
[5] M. Büttiker, Y. Imry and R. Landauer, Phys. Lett. **96** A365 (1983).
[6] G. Montambaux, H. Bouchiat, D. Sigeti and R. Friesner, Phys. Rev. B **42**, 7647 (1990).
[7] B.L. Altshuler, Y. Gefen, and Y. Imry, Phys. Rev. lett. **66**, 88 (1991).
[8] A. Schmid, Phys. Rev. Lett. **66**, 80 (1991).
[9] F. Von Oppen and E. K. Riedel, Phys. Rev. Lett. **66**, 84 (1991).
[10] U. Eckern and A.Schmid, Europhys. Lett. **18**, 457 (1992).

[11] A. Mueller-Groeling, H.A. Weidenmuller and C.H. Lewenkopf, Europhys. Lett. **22**, 193 (1993).
[12] R.Haydock, V.Heine and M.J. Kelly, J. Phys. C **8**, 2591 (1975).
[13] G. Bouzerar, D. Poilblanc and G. Montambaux, Phys. Rev. B **49**, 8258 (1994); see also R. Berkovits, Phys. Rev. B **48**, 14381 (1993).
[14] H. Kato and D. Yoshioka, Phys. Rev. B **50**, 4943 (1994).
[15] J.M. Kosterlitz and D. Thouless, J. Phys. C **6**, 1181 (1973).
[16] A. Doty and D.S. Fisher, Phys. Rev. B **45**, 2167 (1992).
[17] G. Bouzerar and D. Poilblanc, J. Phys. I **4**, 1699 (1994).
[18] K.J. Runge and G.T. Zymanyi, Phys. Rev. B **49**, 15212 (1994).
[19] T. Giamarchi and B.S. Shastry, Phys. Rev. B **51**, 10915 (1995).
[20] W. Deng et al., Phys. Rev. B **50**, 7655 (1994).
[21] H. Mori and M. Hamada, SISSA cond-mat/9509069 preprint.
[22] G. Chiappe, J.A. Verges and E. Louis, SISSA cond-mat/9603153 preprint.
[23] G. Bouzerar and D. Poilblanc, Phys. Rev. B **52**, 10772 (1995).
[24] G. Bouzerar and D. Poilblanc, SISSA cond-mat/9512153 preprint.
[25] H. Bouchiat and G. Montambaux, J. Phys. (Paris) **50**, 2695 (1989); see also Ho-Fai Cheung et al., Phys. Rev. B **37**, 6050 (1988).
[26] H. Bouchiat, G. Montambaux and D. Sigeti, Phys. Rev. B **44**, 1682 (1991).
[27] V. Ambegaokar and U. Eckern, Phys. Rev. Lett., **65**, 381, (1990); see also G. Montambaux, J. Phys. I **6**, 1 (1996).
[28] M. Ramin, B. Reulet and H. Bouchiat, preprint (1994).
[29] P.D. Kirkman and J.B. Pendry, J.Phys. C, **17**, 4327 (1984). M. Kappus and F.J. Wegner, Z. Phys. B **45**, 15 (1981).
[30] R. Berkovits and Y. Avishai, Europhys. Lett. **29**, 475 (1995).

COURANTS PERSISTENTS DANS LES SYSTÈMES DE FERMIONS CORRÉLÉS

Les courants persistents dans des anneaux mésoscopiques désordonnés sont étudiés à l'aide de méthodes de diagonalisations exactes à 1D et de méthodes Hartree-Fock auto-cohérentes à 2D. Dans le cas unidimensionnel d'un modèle de fermions sans spin, les interactions électroniques augmentent toujours la localisation. En revanche, dans le cas de sytèmes bi-dimensionnels de fermions avec spin 1/2, le courant permanent est nettement augmenté par les corrélations électroniques. Il est montré que ce phénomène est intrinsèquement lié à la diminution des inhomogénéités de densité de charge dans l'espace provoquée par les interactions électroniques. Cette étude démontre l'importance cruciale des degrés de liberté de spin.